International Journal of Applied Earth Observations and Geoinformation 106 (2022) 102664

Contents lists available at ScienceDirect

International Journal of Applied Earth Observations and Geoinformation

journal homepage: www.elsevier.com/locate/jag

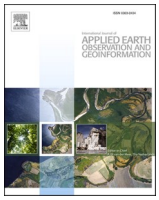

Classifying land-use patterns by integrating time-series electricity data and high-spatial resolution remote sensing imagery

Yao Yao [a,b,1], Xiaoqin Yan [a,1], Peng Luo [c,*], Yuyun Liang [a,*], Shuliang Ren [a], Ying Hu [a], Jian Han [d], Qingfeng Guan [a,b]

[a] School of Geography and Information Engineering, China University of Geoscience, Wuhan, Hubei 430078, China
[b] National Engineering Research Center of GIS, China University of Geoscience, Wuhan, Hubei 430074, China
[c] Chair of Cartography and Visual Analytics, Technical University of Munich, 80333 Munich, Germany
[d] State Grid Pingxiang Power Supply Company, Pingxiang, Jiangxi 337000, China

ARTICLE INFO

Keywords:
Urban land-use classification
Time-series electricity data
High-spatial resolution images
Feature fusion
Deep learning
TR-CNN

ABSTRACT

Accurate identification of urban land-use patterns is essential to rational optimization of urban structure. By combining the external physical characteristics of city parcels obtained from remote sensing images and the socioeconomic attributes revealed by social sensing data, land use can be better classified. However, most of the existing social sensing data have location bias and lack temporal resolution, which cannot accurately reflect the socioeconomic information of land use and leads to low classification accuracy. Based on the above problems, this study explores the deep semantic information of high-spatial and temporal resolution time-series electricity data to explore its relationship with socioeconomic attributes and construct a neural network (TR-CNN) that can fuse time-series electricity data and remote sensing images to identify urban land-use types. We selected Anyuan District in Pingxiang City, Jiangxi Province for a demonstration study, and the results show that the accuracy of the proposed model is 0.934, which is 4.3% and 6.7% higher than that of the ResNet18 model using only remotely sensed images and the LSTM-FCN model using only time-series electricity data. The results also show that the use of time-series electricity data can effectively identify residential and commercial areas, but it is difficult to identify public service facilities compared with remote sensing images. This study finds for the first time that the semantic features of electricity data can fully reflect socioeconomic attributes and can accurately perceive urban land-use patterns from both "top-down" and "bottom-up" recognition patterns by coupling remote sensing images and electricity data.

1. Introduction

Complex land-use types, including residential, commercial, and public facilities, have developed in cities with the urbanization process (Xia et al. 2020, Zhang et al. 2017). Land uses are closely related to human activities and can effectively reflect regional socioeconomic attributes (Jiang et al. 2015, Ye et al. 2021). Therefore, accurate perception of urban land space structure and effective urban land-use classification is an important part of current urban spatial planning (Crooks et al. 2015, Han et al. 2020, Hersperger et al. 2018), which helps the government in decision-making and management.

Remote sensing images are widely used in land-use classification given their ability to capture the physical attributes of cities such as shape and texture (Li et al. 2020, Rogan and Chen 2004, Zhang et al. 2014). Previous studies have demonstrated that an object-oriented approach is an effective method for land-use classification from remote sensing images (Blaschke 2013, Li et al., 2014a, 2014b). However, this method can only mine the shallow land cover information, ignoring the ground's spatial distribution and semantic features. Deep learning offers the possibility to efficiently identify land-use studies with powerful visual representations of images (Kussul et al. 2017, Yuan et al. 2020). For example, Liu and Shi (2020) used convolutional neural networks (CNNs) for land-use classification based on remote sensing images. This study verified that neural networks with deep architecture can

* Corresponding authors.
E-mail addresses: yaoy@cug.edu.cn (Y. Yao), xxxiaoqin@cug.edu.cn (X. Yan), peng.luo@tum.de (P. Luo), 20161000196@cug.edu.cn (Y. Liang), renshuliang@cug.edu.cn (S. Ren), hhying@cug.edu.cn (Y. Hu), guanqf@cug.edu.cn (Q. Guan).
[1] These authors have equal contributions.

https://doi.org/10.1016/j.jag.2021.102664
Received 26 October 2021; Received in revised form 9 December 2021; Accepted 22 December 2021

extract accurate image features to obtain better classification results. However, remote sensing images can only characterize the external physical attributes of cities from the top down and cannot distinguish some land-use types with similar features (Feng et al. 2021). It is necessary to combine multisource data to compensate for the shortage of remote sensing images for land-use classification.

The emergence of social sensing data has brought new opportunities for land-use classification. With the development of information technology, there are increasingly big data that record human activities, such as check-in data (Shen and Karimi 2016), POI data (Yao et al. 2017), taxi data (Du et al., 2020a, 2020b), and cell phone signaling data (Zhang et al. 2021). Social sensing data can be used to extract socioeconomic attributes of land use "from the bottom up" (Yang et al. 2019, Zhan et al. 2014). Given the strong relationship between land use and socioeconomic activities, some studies have used social sensing data for land-use classification (Yao et al. 2021). Among them, deep learning methods have been proven to effectively extract land-use features from social sensing data (Srivastava et al. 2020, Yao et al. 2018). For example, Huang et al. (2018a, 2018b) extracted spatiotemporal features such as the location and time of Twitter data based on latent Dirichlet allocation (LDA) and long short-term memory (LSTM) to classify land use, demonstrating the effectiveness of deep learning to extract features of temporal data.

Based on the external physical attributes of land-use units reflected by remote sensing images and the socioeconomic information reflected by social media data, some scholars have attempted to fuse the two to compensate for the lack of single data features (Cao et al. 2020, Su et al. 2021, Zhang et al. 2019). For example, Liu et al. (2017) identified urban land-use types at the level of traffic analysis zones by fusing high-resolution remote sensing imagery and social media data based on probabilistic topic models and support vector machines (SVMs). The method considers both the physical and socioeconomic characteristics of cities, but the data feature extraction capability based on shallow machine learning is limited and cannot fully exploit the nonlinear features in the data. He et al. (2021) proposed a CF-CNN dual-stream neural network to simultaneously process remote sensing images and Tencent real-time population density data to analyze urban mixed land use, demonstrating the use of deep learning techniques to mine multisource data features to more accurately analyze land use. However, traditional social perception data cannot accurately reflect the activity behavior of all regions and populations due to two limitations, location bias and nontime series (Guan et al. 2021). The errors caused by these limitations are difficult to be eliminated even by coupling remote sensing images. In addition, data fusion is challenging due to the differences in the scale, structure and quality of multisource data. Therefore, feature extraction methods and fusion strategies need to be developed for different data forms to better extract data features (Yin et al. 2021).

Municipal service data, such as time-series water or electricity data provided to residents, have the advantages of high-spatial and temporal resolution, comprehensive coverage of population and socioeconomic activities, and long-time span compared to emerging big data where bias exists (Villar-Navascués and Pérez-Morales 2018). Among them, time-series water data have been shown to be applied in urban land-use studies by sensing socioeconomic attributes (Guan et al. 2021, Pan et al. 2020). Time-series electricity data, as municipal service data, include specific granularity and wide coverage, and they are higher temporal resolution than time-series water data (Chen et al. 2018). Therefore, time-series electricity data provide potential possibilities for analyzing land use at a fine scale. However, few studies have explored the correlation with land use by mining electricity temporal features through deep learning.

In summary, previous studies have proven that remote sensing images can reflect the external physical attributes of cities, and municipal service data can perceive the socioeconomic attributes of cities. However, due to the lack of relevant data and models, few studies have attempted to mine the features of time-series electricity data and remote sensing images for urban land-use analysis simultaneously. Therefore, we proposed the following scientific question: can we identify urban land-use types by exploring the relationship between deep semantic information and socioeconomics in time-series electricity data and coupling remote sensing image data? In this study, ResNet18 and LSTM-FCN were introduced to construct a feature fusion neural network (TR-CNN). The main urban zone of Pingxiang City, Jiangxi Province, was selected as the study area. Remote sensing images and time-series electricity data were processed in TR-CNN to verify the validity of fusing the external physical attributes and the socioeconomic attributes for land-use classification. Finally, we analyzed the land-use distribution patterns of the study area revealed by the TR-CNN.

The remainder of this paper is presented below. Section 2 describes the study area and data. Section 3 covers the methodologies to classify the land use pattern proposed in this study. Section 4 validates the proposed method and present the results of this study. In Section 5, we discuss the contributions the current limitations of this study. Finally, the study is concluded in Section 6.

2. Study area and data

Pingxiang City (Fig. 1 (A2)) is an essential region of the middle reaches of the Yangtze River Delta urban agglomeration in China and is the center of economic development in western Jiangxi Province (Fig. 1 (A1)), with a resident population of 1,804,805 and a regional GDP of 96.360 billion (Statistics Bureau of Pingxiang). Pingxiang City has formed complex and diverse land-use types due to the rapid growth of population and economy. The study area (Fig. 1 (A3)) is located in the central city of Anyuan, which is the political, economic, and cultural center of Pingxiang City. The study area has established perfect municipal infrastructure services, with an area of 24.25 km^2. Remote sensing data and user time-series electricity data were used for land-use classification. The high-resolution remote sensing image in 2020 was downloaded from Google Earth, which contains three bands (red, green, blue) with a spatial resolution of 0.60 m. The remote sensing image was uniformly segmented into 96 $\times$ 96 pixel subsets for subsequent model input.

In this study, user time-series electricity data were used to reveal the socioeconomic attributes of land use. There are two different power supply transformers, public transformers and dedicated transformers. Public transformers are commonly used to supply power to general residents and low-voltage nonresidents (e.g., small- and medium-sized commercial and service facilities), while dedicated transformers are used to meet high-demand users such as industrial users (Queiroz et al. 2020). Limited by the data availability, only the public transformer electricity data provided by the State Grid Pingxiang Power Supply Company (Fig. 1(B)) are used in this study. Hence, the selected study area does not include the industrial area. The daily electricity data cover 127 days from September 15, 2020, to February 8, 2021. Each electricity dataset contains information such as an address, customer number and name, type of electricity consumption, and daily electricity consumption. The user address information is converted to the user's latitude and longitude information through Baidu API geocoding.

3. Methodology

We construct a feature fusion neural network based on deep learning to identify urban land-use classes by coupling time-series electricity data with remote sensing images. The research process consists of three main parts (Fig. 2): (1) Data preprocessing. Data cleaning and enhancement were conducted for two datasets: time-series electricity data and remote sensing data. They are spatially matched in each sample. (2) Construct the feature fusion neural network (TR-CNN) to analyze the effectiveness of fusing time-series electricity data and remote sensing images features for urban land-use identification. (3) Identify land-use types of each grid parcel based on TR-CNN. In addition, to verify the effectiveness of the

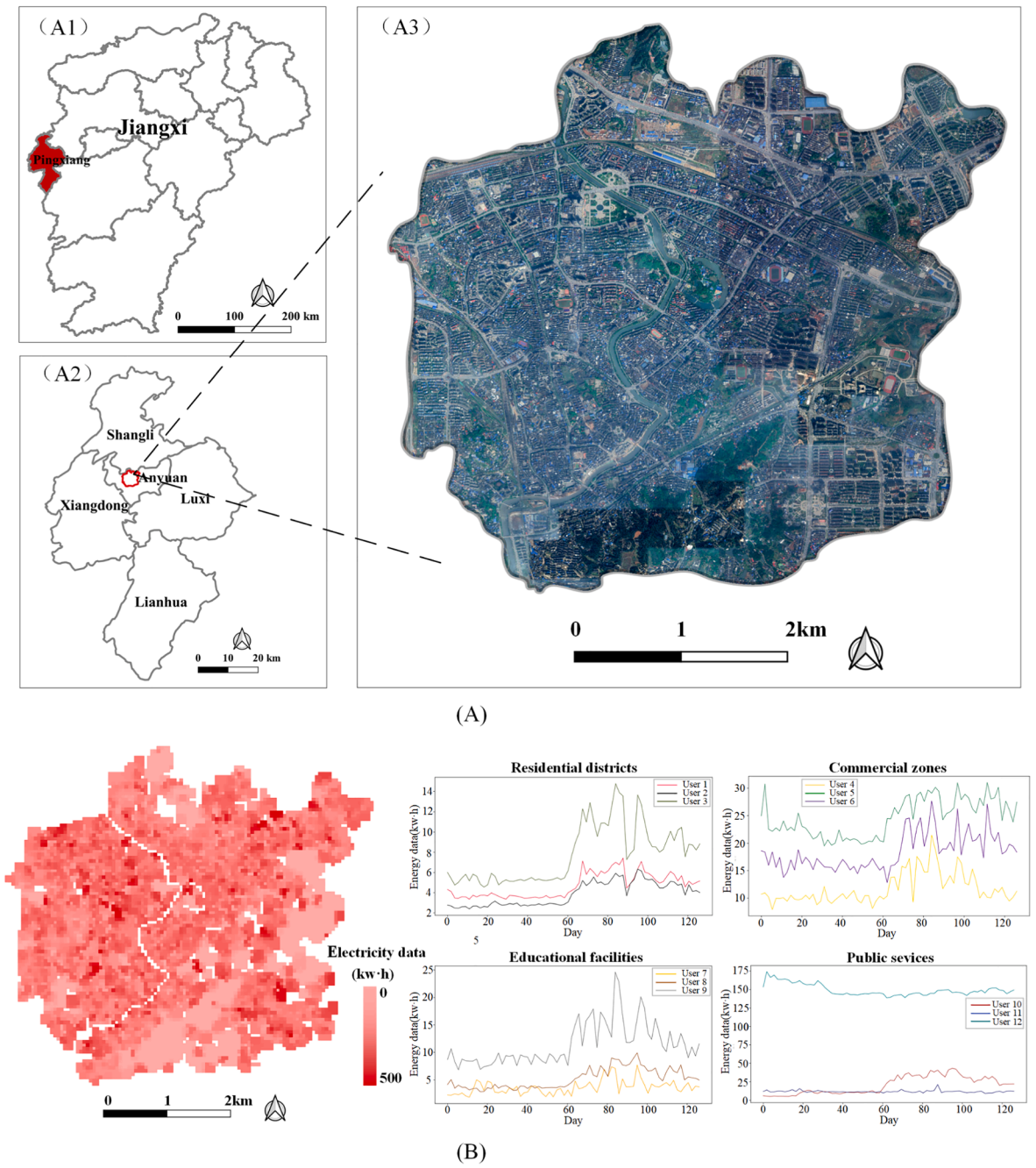

Fig. 1. Overview of the study area. (A) Case study area: (A3) The central city of Anyuan District is located in (A2) Pingxiang city and (A1) Jiangxi Province. (B) Overall electricity data and some samples collected in the study area. Electricity data of the green land are manually set to 0.0001 (converging to 0) every day.

proposed model, we conduct a comparative analysis with a single data model and conduct ablation experiments on the model.

3.1. Data cleaning and enhancement

Since there are more missing values in the original time-series electricity data, data cleaning is necessary. In this study, the 80% rule is used to remove the user samples with more than 20% missing sequences in the electricity data, and the remaining sequence missing values are filled with the average value of the sequence (Bijlsma et al. 2006).

The study area was divided into grid plots of the same size as the image blocks to facilitate the spatial matching of remotely sensed images with the electricity data. The electricity data used in this study is point data, but it represents the electricity consumption of an area (e.g., an office building). If the electricity point data is located within a block with a corresponding remotely sensed image, it is spatially correlated with the image block. In addition, we conducted the 20-m buffer of electricity point data in the grid plots. Because 20 m is usually regarded as the standard scale of buildings in the previous studies (Hossain 2021, Li et al., 2014a, 2014b). When the grid overlapped with the buffer, we averaged the electricity data of the overlapped portion with the electricity data of the original grid. We used it as the electricity data value of that grid. The buffer analysis is also expected to solve the address offset problem converted by Baidu API.

The original electricity data were labeled with some rough categories, including urban residential, commercial, educational, non-residential, and non-industrial. However, some misclassifications in the original data make it difficult to determine the exact electricity

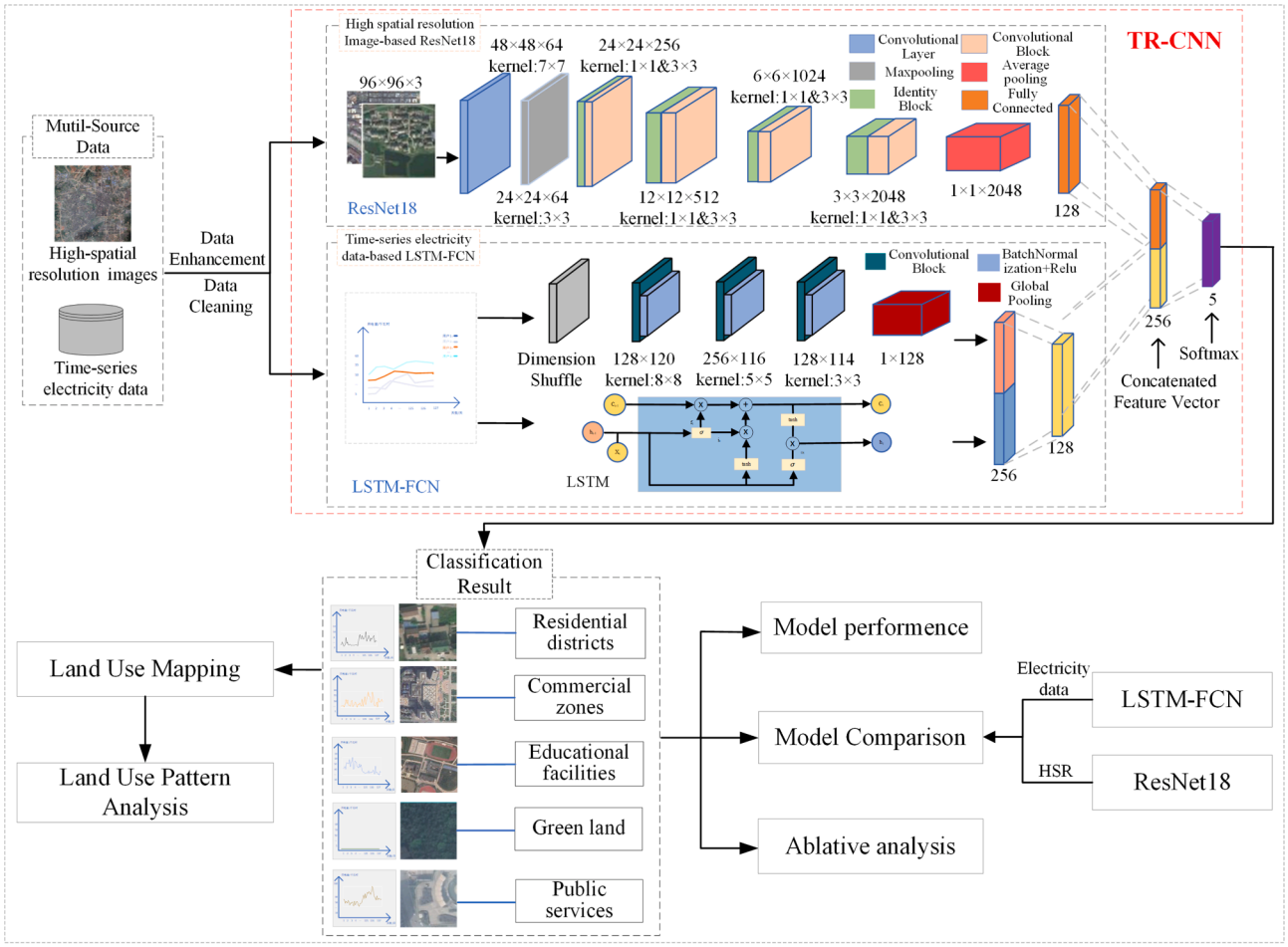

Fig. 2. The workflow of urban land-use classification.

category of customers in the original labels. For example, several residential areas were labeled as commercial electricity use. Therefore, the correction of labels is necessary. On the basis of labels in electricity data, we re-labeled the land-use pattern by combing remote sensing data and expert experience. The electricity consumption category of each user was reclassified into four categories: residential, commercial, public service facilities, and educational facilities (He et al., 2021, Huang et al., 2018a, 2018b). The user electricity data used in this study are distributed in built-up areas, which cannot be applied to analyze the socio-economic attributes in nonbuilt-up areas. However, the study area is located in a hilly area with extensive vegetation coverage. To ensure the integrity of the study area coverage as much as possible, we keep the green areas and assumed their electricity consumption to be 0.0001 (converging to 0). Each sample label is settled before the model training. For each sample, green land is labeled by remote sensing data first, and other land-use types are labeled by the type of electricity consumption with the largest proportion. Finally, we check and correct each sample by combing remote sensing images and expert experience.

After sample labeling, 80% of the samples are randomly selected as the training set, and the remaining 20% are selected as the test set. To enhance the generalization ability of the model while avoiding overfitting, the obtained sample sets are subjected to data enhancement separately. Rotation, contrast stretching, and gamma transform are used for data enhancement of remote sensing images (Tasar et al. 2019). Meanwhile, this study used a weighted form of Dynamic Time Warping (DTW) Barycentric Averaging technique for data enhancement of time-series electricity data (Fawaz et al. 2018). The method first randomly selects a time series and assigns a weight of 0.5 to it. Then the two most similar time series are selected based on DTW and given 0.15 weight each, and the remaining time series are equally weighted by 0.2. Finally, the average of each timestamp of each time series is calculated based on the weights as the value of the new time series. To facilitate the correlation of different data in each land-use type sample, the number of remote sensing image samples and time-series electricity data sample enhancement in each land-use sample are kept consistent. Considering the limited original samples, we randomly match the enhanced time-series electricity data and remote sensing images in different categories to expand the sample combinations. This allows the model to learn the rich combination of features in the same category as randomly as possible and improves the model generalization.

3.2. Urban land-use classification based on TR-CNN model

The overall structure of the proposed TR-CNN model is shown in the red dashed box in Fig. 2, which consists of the ResNet18 network and the LSTM-FCN network. Specifically, considering the data heterogeneity, we select ResNet18 to extract features from high-resolution remote sensing images and LSTM-FCN to extract features from time-series electricity data. Both datasets were processed into 128-dimensional feature vectors and then further stitched into 256 dimensions. Finally, the feature vector with 256 dimensions was inputted to the fully connected layer and softmax classifier to obtain classification results.

3.2.1. ResNet based feature extraction from remote sensing images

In this study, to prevent overfitting due to model complexity, we choose ResNet18 based on the basic block to construct a high-dimensional feature extraction model for remote sensing images (Schaetti 2018). The ResNet network proposed by He et al. (2016) was

proven to be effective in alleviating the neural network gradient explosion problem and has excellent performance on image classification. As shown in Fig. 3, the residual block, as the core of the ResNet network, can connect the output data of the previous layer to the input data of the latter layer by jumping multiple layers, thus passing the information to deeper layers of the neural network and extracting richer features of the remote sensing image data.

Remote sensing images are first input to the 7 × 7 convolutional layer and the 3 × 3 maximum pooling layer. Then, the output image feature maps are transferred to each group of residual blocks and simplified into feature vectors by the global pooling layer. To facilitate the stitching of multisource data features, it is finally modified to 128 dimensions through the fully connected layer as the final extracted remote sensing image features.

3.2.2. LSTM-FCN-based feature extraction from time-series electricity data

Since there are significant differences in data structure between time-series data and remote sensing images, the feature extraction methods should also be different. In this study, the LSTM-FCN proposed by Karim et al. (2018) is selected to extract the features of the time-series electricity data. It can better extract temporal information of human activities and is used for feature extraction of socioeconomic attributes. LSTM-FCN includes the FCN module and LSTM module, which perceive the same temporal data in two different views. In the FCN module, the time-series data are regarded as univariate time series with multiple time steps and input to three temporal convolution blocks for feature extraction, and then the feature vectors are obtained by a global average pooling layer. LSTM converts multilength univariate time data into multivariate time series with a single time step through the dimensional shuffle (DS) module. The DS module helps LSTM-FCN to extract features of the same timing data in two different formats. The LSTM structure includes input gates, forget gates, and output gates, through which the three gating states control the content of the time-series data transmission to retain important timing information. The data are input to the LSTM module and FCN module for training. Finally, the timing features extracted from the FCN and LSTM modules are stitched together and processed into a 128-dimensional feature vector through the fully connected layer for the next training step.

Since LSTM has been shown to have good performance in processing long time step time-series data (Wang et al. 2020), this study converts the DS module from the LSTM to the FCN to ensure that LSTM can perform better by capturing the semantic association between long sequences. With the DS module, the original electricity data (1 × 127) with 127 time steps in a single variable is converted into a multivariate array (127 × 1) with a single time step. Therefore, the LSTM extracts univariate time-series electricity features with multiple time steps in this study, while the FCN module is used to extract multivariate time-series electricity features with a single time step.

3.2.3. Model comparison and accuracy assessment

Two single models, ResNet18 and LSTM-FCN, are used to conduct the comparison experiments to verify the effectiveness of TR-CNN. To analyze whether multisource data fusion can effectively improve land-use classification accuracy, remote sensing images are input into ResNet18, and time-series electricity data are input into LSTM-FCN. In addition, we conduct ablation experiments to verify the necessity of each part of the model. For time-series feature extraction, we transform or discard the LSTM-FCN modules, including the movement of the DS module, and use only the LSTM or FCN modules in LSTM-FCN for training. For remote sensing image feature extraction, we replace ResNet18 with VGG16 or AlexNet to analyze the performance of ResNet18 in TR-CNN.

The confusion matrix, test accuracy and Kappa coefficient are used as model evaluation metrics. The test accuracy and Kappa coefficient are calculated as:

$$Test\ \ Accuracy = \frac{\sum_{i=1}^{n} x_{ii}}{N} \tag{1}$$

$$Kappa = \frac{\sum_{i=1}^{n} x_{ii}/N - \sum_{i=1}^{n}\left(\sum_{j=1}^{n} x_{ij}\sum_{j=1}^{n} x_{ji}\right)/N^2}{1 - \sum_{i=1}^{n}\left(\sum_{j=1}^{n} x_{ij}\sum_{j=1}^{n} x_{ji}\right)/N^2} \tag{2}$$

where x_{ij} is the elements of the i-th row and j -th column of the confusion matrix, x_{ii} is the correctly predicted samples, n is the number of categories, and N is the number of test samples.

4. Results

4.1. Validation of the TR-CNN model

In this study, 526 original samples were obtained after data preprocessing. After data enhancement, 4,544 samples were obtained, 1,424 were residential areas, 1,288 were commercial areas, 288 were educational facilities, 1,160 were green areas, and 384 were public service facilities. All experiments were run under the PyTorch framework with Python 3.6 and accelerated with a GTX 1070 6G GPU. The learning rate, number of iterations, and batch size of all models were set to 0.0001, 100, and 16, and the network was trained with the Adam optimizer and cross-loss function to optimize the objectives. To prove the model validity and reliability, 20% of the training set data were randomly selected as validation data. And this process repeated 10 times. Validation results showed that the model has strong reliability with small error fluctuations (test set error $< \pm 0.05$). We select the model hyperparameter set with the highest accuracy and fine-tune it on all training sets to obtain the final model parameters for further experiments.

Fig. 4 represents the changes of loss and precision for the three models over 100 iterations. The training accuracy of LSTM-FCN and ResNet18 gradually reaches 0.943 and 0.958 after about 60 iterations,

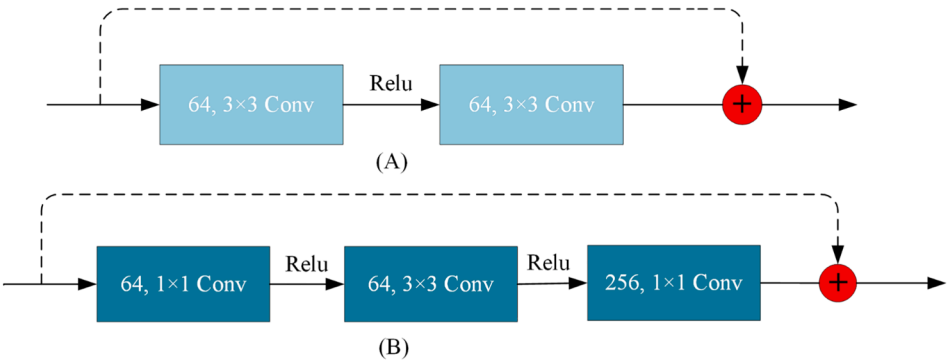

Fig. 3. Residual block types. (A) basic block for ResNet-18/34. (B) bottleneck block for ResNet-50/101/152.

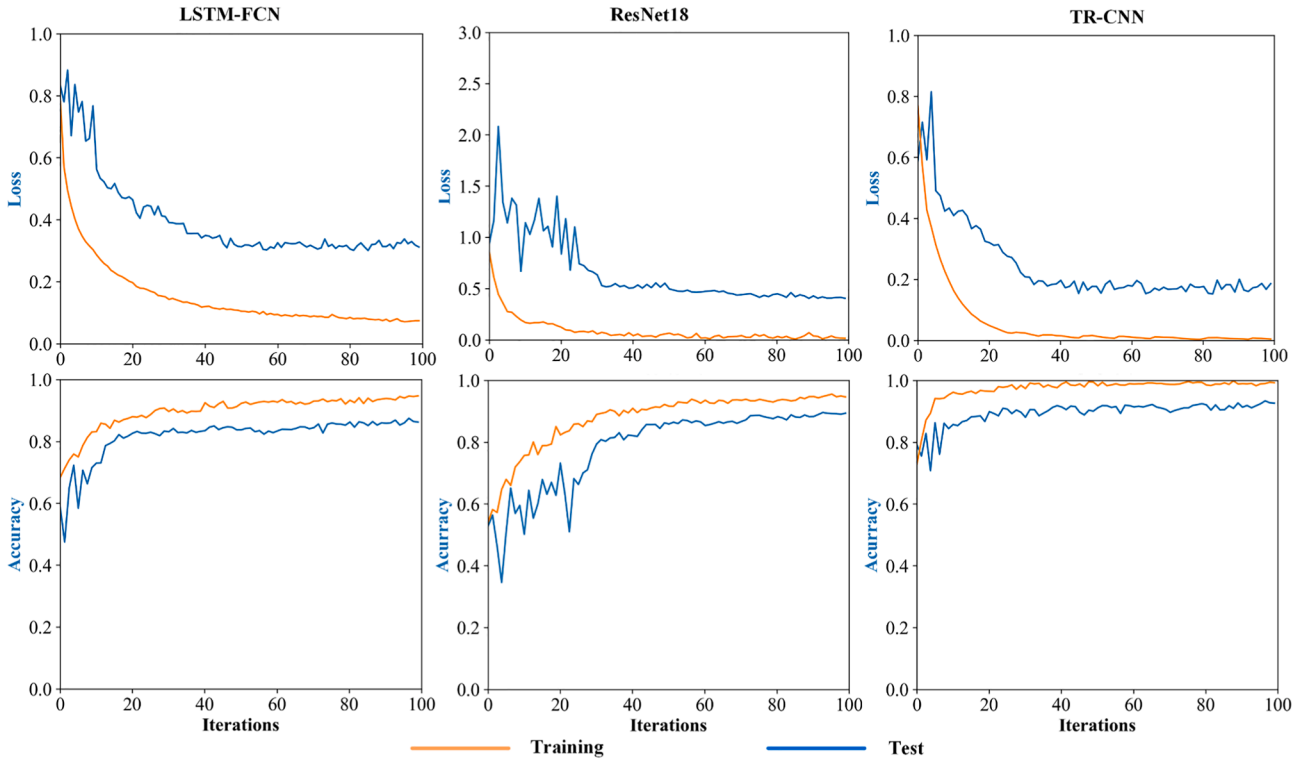

Fig. 4. Accuracy and loss values for the training and test sets of the three models.

while the training accuracy of TR-CNN approaches 1.0 after about 30 iterations. In addition, we choose cross-entropy as the loss function, and the results show that the training loss and test loss curves show an oscillating trend in the early stage and gradually decrease with model optimization, and both converge after 50 iterations. There is no obvious overfitting phenomenon during the training process. Table 1 shows the training results of the three models, and the TR-CNN model obtained the optimal performance with a test accuracy of 0.934 and a Kappa of 0.912. The test accuracy and Kappa of ResNet18 for extracting remote sensing image features were 0.895 and 0.859, respectively, and the test accuracy and Kappa of LSTM-FCN for extracting temporal electricity features were 0.875 and 0.831, respectively.

From the confusion matrix in Fig. 5, it can be seen that all three models achieved high classification accuracy, but the performance varied for different land-use types. Using the time-series electricity data, LSTM-FCN accurately identified four land-use categories: residential areas, commercial zones, educational facilities, and green land. All of their accuracies reached more than 80%. In particular, the classification accuracy for residential and green areas reached 97% and 100%, respectively. This result is reasonable because residential areas have a relatively regular electricity consumption pattern, and the electricity consumption curve of green land is smooth and easy to identify since they are set artificially by the experiment. However, public service facilities were poorly identified by LSTM-FCN, with an accuracy of only 48%. This may be because public service facilities contain several different categories with large variances in electricity consumption. It is not easy to extract the time-series pattern from hospitals, police stations, and neighborhood councils that have large differences effectively.

Table 1
Performance of our approach with comparative models.

Model	Input Data	Test Accuracy	Kappa
LSTM-FCN	Electricity data	0.875	0.831
ResNet18	HSR	0.895	0.859
TR-CNN	Electricity data + HSR	0.934	0.912

The results show that ResNet18 effectively identified residential areas, educational facilities, and green areas from remote sensing images, and the accuracy of green areas was 100%. In contrast, the recognition accuracy in commercial and public service facilities was lower, only 74% and 66%, respectively. ResNet18 accurately extracted the image features of green areas and educational facilities, but it was difficult to recognize commercial areas compared to LSTM-FCN, which may be due to the existence of complex and confusing building structures in commercial areas.

Compared with those two models, which only use a single data source, the TR-CNN model proposed in this study performs excellently in urban land-use identification. Fusing remote sensing images with electricity data significantly improved the identification accuracy of residential areas, commercial areas, and educational facilities, all of which are up to 90%. However, it is worth noting that for public service facilities containing several categories, electricity consumption also varied greatly, so the accuracy was relatively low even after data fusion.

Several typical regions were selected for error analysis of the three models (Fig. 6). Areas without significant electricity consumption patterns were difficult to recognize by the LSTM-FCN model. However, since they have obvious physical features, such as regular building structures (Fig. 6A) and basketball courts (Fig. 6B), remote sensing images can be used to avoid incorrect classification using time-series electricity data. In contrast, some areas without significant shapes or textures were hard to recognize by remote sensing images. Electricity patterns can be extracted and help to recognize their land use. For example, Fig. 6(C) shows a commercial area located near the political center of the study area, which was influenced by the construction plan, making it similar to residential buildings. Fig. 6(D) shows a public square in a community circle, which is similar to a commercial shopping center from the remote sensing image. Fig. 6(E) shows a large farmers' market, which has typical commercial electricity characteristics, but the image characteristics are similar to those of an urban village. As the image features of these three parcels were easily confused with other classes, their electricity consumption curves are obvious, and the correct classification results were obtained by fusing the time-series electricity

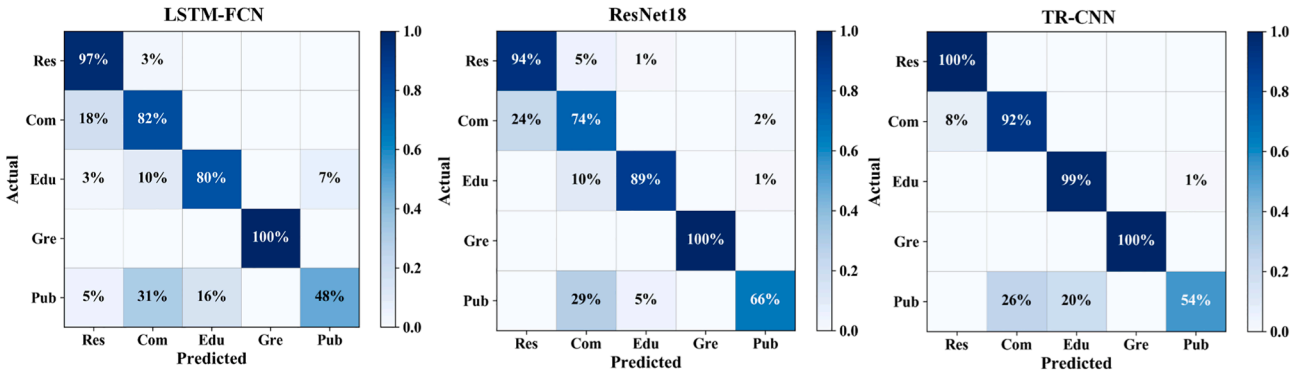

Fig. 5. Confusion matrix for the three models. Types of land use: Res = residential districts, Com = commercial zones, Edu = educational facilities, Gre = green land, and Pub = public services.

features.

However, complex scenarios cannot be correctly predicted even by fusing multiple source features. Fig. 6(F) shows the city museum, which is similar to the commercial building from the remote sensing image and had no obvious electricity consumption pattern, and the correct classification result could not be obtained even after feature fusion. In summary, our results show that features can be compensated between multiple sources of data to achieve more accurate land-use classification results than a single data source.

4.2. Ablation study

For the two temporal feature extraction modules and image feature extraction included in TR-CNN, this study performed an ablation analysis to verify the effectiveness and necessity of each module. The results of the ablation experiments are shown in Table 2. To analyze the effect of the location of the dimensional shuffle (DS) module on the performance of the LSTM-FCN model, we adjusted the DS component to the front of the LSTM, i.e., the LSTM treats the time-series data as multivariate time series and the FCN treats the time-series data as univariate time series, forming Model 2, which has a decreased model performance. This implies that the performance improvement of the DS module for FCN was greater than that of LSTM, and the further ablation experiments all put the DS module in front of FCN by default. In addition, to verify the LSTM-FCN time-series feature extraction capability, we only used LSTM (Model 3) or FCN (Model 4) for electricity data classification, and this approach also degraded the model performance.

We replaced ResNet18 with VGG16 and AlexNet to form Model 5 and Model 6, respectively. ResNet18 used in TR-CNN obtained the optimal performance by virtue of the excellent feature recognition ability of residual blocks. We found that although the performance of the fusion model using VGG16 or AlexNet was slightly lower, its accuracy was also significantly higher than that using single time-series electricity data or remote sensing images. This implies that from the perspective of model feature extraction, the use of multisource data fusion is superior to the method using only single data. The results demonstrate that each module of TR-CNN is a necessary component to obtain optimal land-use classification results.

4.3. Land-use patterns analysis

The land-use mapping in the study area was performed using the proposed TR-CNN model, and the results are shown in Fig. 7. The study area was staggered with residential and commercial-oriented distribution, and educational facilities and public services were relatively balanced across the area to facilitate residents' access to various services. We analyzed the socioeconomic attributes of the study area according to the proportion of each land-use type. The commercial and residential dominated areas occupied 48.7% and 26.9% of the study area, respectively, consistent with the phenomenon that most urban residential and commercial areas were mainly concentrated in the main city. Green areas dominated by ecological parks and forests were mainly distributed in the southeastern part of the study area, occupying 15.2% of the study area. This phenomenon was reasonable, as the residents' demand for the ecological environment gradually increased with the quality of life improvement, and in addition, Pingxiang City, as a typical southern Chinese region, has high natural vegetation coverage. Public service facilities and educational facilities have scattered distributions, accounting for 5% and 4.2%, respectively. Such facilities are influenced by residents' travel and have a close spatial relationship with residential areas.

The ratio of different land uses obtained from our results was generally consistent with the Chinese urban planning technical standards (Long et al. 2020). The only difference was that the proportion of commercial zones calculated in this study is higher than residential area. The study area was located in the economic center of Pingxiang City with a large amount of commercial land. In addition, with the development of the social economy and transportation, residents gradually move to the suburbs to seek a more comfortable living environment, thus leading to a decrease in residential areas in urban centers. The above analysis shows that the proposed TR-CNN model can effectively identify urban land-use types, and the mapping result can deepen our understanding of the distribution of urban land functions.

5. Discussion

5.1. Effectiveness of TR-CNN model

Due to the lack of relevant data and models, few studies have explored the relationship between time-series electricity data and socioeconomic attributes and used it for urban land-use analysis. To solve this problem, the structural differences between remote sensing images and time-series electricity data were considered in this study, and a deep learning-based TR-CNN model for land-use classification was developed by fusing the features from these two datasets. The results show that compared with ResNet18 (Test accuracy: 0.895, Kappa: 0.859) using remote sensing images and LSTM-FCN (Test accuracy: 0.875, Kappa: 0.831) using time-series electricity data, the TR-CNN model proposed in this study obtained optimal performance (Test accuracy: 0.934, Kappa: 0.912).

We verified the necessity of each module of TR-CNN by ablation analysis. By inputting temporal electricity data into the LSTM-FCN model, we found that multivariate time series with a single time step can significantly improve the FCN performance, while LSTM is more suitable for extracting sequence features with multiple time steps. This method reveals the mode of FCN and LSTM perceiving time-series data and provides a reference for future research. In the remote sensing image feature analysis, it was shown that the performance of VGG16 was only

Fig. 6. Error analysis of the land-use classification results. The ground truth of examples. (A) Kangyuan community. (B) Dengan primary school. (C) Office building. (D) Lvyin square. (E) Farmer's market. (F) Pingxiang museum. The red font indicates that the model predicts correctly, while black indicates incorrectly.

approximately 1% lower than that of the more advanced ResNet18. Due to the rapid development of artificial intelligence in recent years, deep learning models in image recognition have gradually entered a stable period (Marcus 2018). The performance improvement of the approach by changing the model structure is smaller compared to data fusion. This suggests that future research could focus on extracting richer features from multisource data to improve accuracy.

Our results show that the TR-CNN model significantly improves the

Table 2
Results of the ablation study. The components that are replaced are shaded, and test accuracy and Kappa are used as the model evaluation criteria.

No	Time-series electricity data	HSR	Test accuracy	Kappa
1 (Proposed in this study)	LSTM-FCN	ResNet18	0.934	0.912
2	LSTM(DS)-FCN	ResNet18	0.920	0.893
3	LSTM	ResNet18	0.914	0.885
4	FCN	ResNet18	0.902	0.870
5	LSTM-FCN	VGG16	0.921	0.898
6	LSTM-FCN	AlexNet	0.907	0.876

classification accuracy for residential, commercial, and educational facilities. This may be because these three land-use types show high consistency in intra-class electricity usage patterns or texture features. However, due to the existence of different building structures and electricity consumption for different functions of public service facilities, the recognition accuracy using single remote sensing images or time-series electricity data was relatively low. In this case, feature fusion complicated the distribution of categories over the feature space, thus expanding the range of model misclassification, resulting in failure to improve the accuracy of public service facility recognition (Ghamisi et al., 2017). Overall, the results show that the integration of the socioeconomic attributes revealed by electricity data and the external physical attributes revealed by remote sensing images can reflect both "bottom-up" and "top-down" characteristics, eliminating the one-sidedness of a single data source and thus effectively improving the accuracy of urban land-use classification.

5.2. Time-series electricity consumption reflecting urban land-use patterns

Our results show that the semantic features of time-series electricity data mined based on deep learning can effectively reflect the socio-economic attributes of different land-use categories, especially the areas with high human socio-economic activities. Although the testing accuracy of the LSTM-FCN model based on electricity data is slightly lower than the overall accuracy of the ResNet18 model based on remote sensing images, the electricity data can better identify residential and commercial areas. It is difficult to distinguish between commercial and residential areas using remote sensing images because of the similarity of the top features of buildings (e.g., office buildings and high-rise residential buildings) (Du et al., 2020a, 2020b). However, there are differences in electricity consumption and trends between these two land-use types. As shown in Fig. 1(B), the electricity consumption in most residential areas shows a trend of smooth in the first period and a sudden increase in the later period, related to the use of heating equipment in winter, etc. (Billimoria et al., 2021). The difference in electricity consumption allows the model to accurately extract the semantic features of different land use categories in the electricity data, more accurately identifying residential and commercial areas and compensating for their limitations of being easily confused on remote sensing images.

Compared to Huang et al. (2018a, 2018b), which used social media data for land-use classification, the time-series electricity data used in this study and the time-series electricity data used by Guan et al. (2021) have the advantages of full group coverage and long time span, avoiding the shortcomings of emerging big data in terms of biased scale and inability to reflect long-term land use. In addition, compared to some social sensing data that can only be available in limited large cities, municipal service data used in this study are the basic data in most regions. Thus, the framework and model proposed in this study provide a new opportunity for land-use classification in small and medium-sized cities worldwide.

5.3. Urban land-use patterns in China's typical developing city

Pingxiang is a typical fast-growing city in China, and understanding its land-use pattern can provide the guide for the development of other cities. We found that the study area has a clear mixed commercial and residential pattern, indicating its growing urbanization process. The central area is the most prosperous area of Pingxiang City, with the largest commercial pedestrian street. In recent years, Pingxiang City has undergone a rapid urban urbanization, and its northern part has gradually formed an economic center. The green areas are in the form of

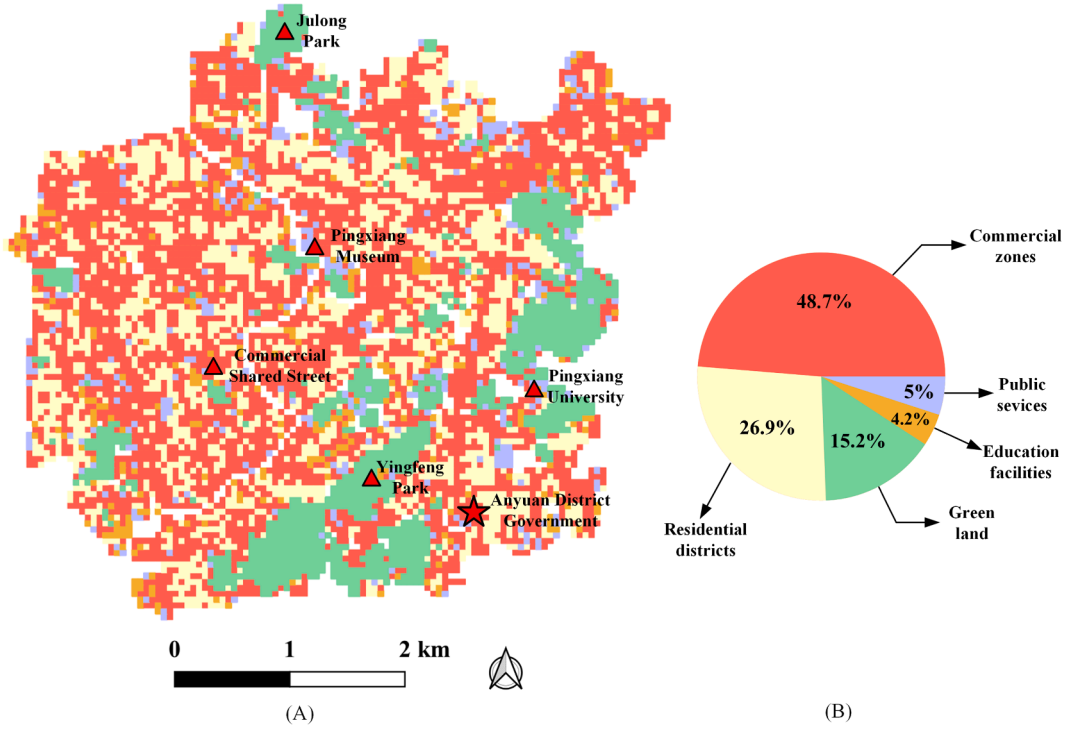

Fig. 7. Spatial distribution of the land-use patterns in the study area. (A) Land-use distribution results. (B) Proportion of each category.

regional aggregation, mainly distributed in the southeast and close to Anyuan National Forest Park. Educational facilities and public services are scattered to facilitate residents' access to public services, which is in line with the "15-minute community living area" planning and construction introduced by most Chinese cities (Weng et al. 2019). The results are similar to the actual situation, proving that TR-CNN can fully exploit the "user behavior-socioeconomic" relationship and "image features-physical properties" relationship with its excellent multisource feature extraction capability, which can be regarded as a reference method to identify land-use patterns for most rapidly growing cities.

5.4. Limitations and future works

There are still shortcomings in this study. First, a uniform grid was selected as the study scale in our study. However, the geographic scale may introduce uncertainty into land-use categories, and the classification results obtained at different scales may differ (Wang et al. 2019). Future studies may conduct a scale sensitivity analysis of land-use classification at multiple scales, including different grid sizes, traffic analysis zones, and administrative boundaries. Second, the behavioral characteristics of users on weekdays, weekends, and holidays should be different (Chen et al. 2017). However, our study did not distinguish them and used time-series electricity data for all days to extract the users' consumption patterns. How to further segment the time-series electricity data for analysis to improve the richness of the dataset becomes the focus of future studies. Thirdly, time-series electricity data cannot extract features for some non-built-up categories, such as bare land (Helber et al. 2019). Future research could consider additional auxiliary data to address more complex scenarios. Fourth, this study only used more common methods such as mean filling for data preprocessing. Future studies can introduce more advanced methods to deal with missing values and thus improve experimental precision.

In addition, two existing efficient models were selected for fusion in this study to verify the effectiveness of time-series electricity data and remote sensing images in identifying urban land use. The innovation of the model is not the primary purpose of this study. The use of deep learning techniques based on multi-source data (or multimodal) has become an essential approach to studying urban land use (Srivastava et al. 2019, Yin et al. 2021). Future research will focus on feature fusion strategies to optimize the models to achieve higher land use classification accuracy.

6. Conclusion

This study confirms that multisource data fusion can effectively identify urban land-use patterns through a deep learning-based feature fusion network (TR-CNN). Since high-resolution remote sensing images can identify only the external physical attributes of cities, this study was the first attempt to mine urban socioeconomic attributes from time-series electricity data through a deep learning model. The TR-CNN model was proposed to identify urban land-use categories by fusing remote sensing images with time-series electricity data. The method was validated in Pingxiang City, and results obtained high test accuracy (0.934) and Kappa value (0.912). The model can fuse "bottom-up" and "top-down" features by coupling socioeconomic attributes with external physical attributes of the city to identify urban land use. It is effective for urban land-use analysis and can accurately reveal the activity intensity in urban buildings. Our study provides an important reference for microscale urban land-use classification and socioeconomic identification.

Funding

This work was supported by the National Key Research and Development Program of China (Grant No. 2019YFB2102903), the National Natural Science Foundation of China (Grant No. 42171466 and 41801306), the Scientific Research Program of the Department of Natural Resources of Hubei Province (Grant No. ZRZY2021KJ02), and China Scholarship Council.

Declaration of Competing Interest

The authors declare that they have no known competing financial interests or personal relationships that could have appeared to influence the work reported in this paper.

References

Bijlsma, S., et al., 2006. Large-Scale Human Metabolomics Studies: A Strategy for Data (Pre-) Processing and Validation. Anal. Chem. 78 (2), 567–574.

Billimoria, S., et al., 2021. The Economics of Electrifying Buildings: How Electric Space and Water Heating Supports Decarbonization of Residential Buildings. In: World Scientific Encyclopedia of Climate Change: Case Studies of Climate Risk, Action, and Opportunity, vol. 3, pp. 297–304.

Blaschke, T., 2013. Object Based Image Analysis: A New Paradigm in Remote Sensing. In: ASPRS Annual Conference, March, 24–28.

Cao, R., Tu, W., Yang, C., Li, Q., Liu, J., Zhu, J., Zhang, Q., Li, Q., Qiu, G., 2020. Deep Learning-Based Remote and Social Sensing Data Fusion for Urban Region Function Recognition. ISPRS J. Photogramm. Remote Sens. 163, 82–97.

Chen, M.o., Ban-Weiss, G.A., Sanders, K.T., 2018. The Role of Household Level Electricity Data in Improving Estimates of the Impacts of Climate on Building Electricity Use. Energy Build. 180, 146–158.

Chen, Y., Liu, X., Li, X., Liu, X., Yao, Y., Hu, G., Xu, X., Pei, F., 2017. Delineating Urban Functional Areas with Building-Level Social Media Data: A Dynamic Time Warping (DTW) Distance Based K-Medoids Method. Landscape Urban Plann. 160, 48–60.

Crooks, A., Pfoser, D., Jenkins, A., Croitoru, A., Stefanidis, A., Smith, D., Karagiorgou, S., Efentakis, A., Lamprianidis, G., 2015. Crowdsourcing Urban Form and Function. Int. J. Geogr. Inform. Sci. 29 (5), 720–741.

Du, S., Du, S., Liu, B.o., Zhang, X., Zheng, Z., 2020a. Large-Scale Urban Functional Zone Mapping by Integrating Remote Sensing Images and Open Social Data. GISci. Remote Sens. 57 (3), 411–430.

Du, Z., Zhang, X., Li, W., Zhang, F., Liu, R., 2020b. A Multi-Modal Transportation Data-Driven Approach to Identify Urban Functional Zones: An Exploration Based on Hangzhou City, China. Trans. GIS 24 (1), 123–141.

Fawaz, H.I., et al., 2018. Data Augmentation Using Synthetic Data for Time Series Classification with Deep Residual Networks. *arXiv preprint arXiv:1808.02455*.

Feng, Y., Huang, Z., Wang, Y., Wan, L., Liu, Y.u., Zhang, Y.i., Shan, X.v., 2021. An SOE-Based Learning Framework Using Multisource Big Data for Identifying Urban Functional Zones. IEEE J. Sel. Top. Appl. Earth Obs. Remote Sens. 14, 7336–7348.

Ghamisi, P., Hofle, B., Zhu, X.X., 2017. Hyperspectral and LiDAR Data Fusion Using Extinction Profiles and Deep Convolutional Neural Network. IEEE J. Sel. Top. Appl. Earth Obs. Remote Sens. 10 (6), 3011–3024.

Guan, Q., Cheng, S., Pan, Y., Yao, Y., Zeng, W., 2021. Sensing Mixed Urban Land-Use Patterns Using Municipal Water Consumption Time Series. Ann. Am. Assoc. Geogr. 111 (1), 68–86.

Han, W., Zhang, X., Zheng, X., 2020. Land Use Regulation and Urban Land Value: Evidence from China. Land Use Policy 92, 104432. https://doi.org/10.1016/j.landusepol.2019.104432.

He, J., Li, X., Liu, P., Wu, X., Zhang, J., Zhang, D., Liu, X., Yao, Y., 2021. Accurate Estimation of the Proportion of Mixed Land Use at the Street-Block Level by Integrating High Spatial Resolution Images and Geospatial Big Data. IEEE Trans. Geosci. Remote Sens. 59 (8), 6357–6370.

He, K., et al., 2016. Deep Residual Learning for Image Recognition. In: In *Proceedings of the IEEE Conference on Computer Vision and Pattern Recognition*, pp. 770–778.

Helber, P., Bischke, B., Dengel, A., Borth, D., 2019. Eurosat: A Novel Dataset and Deep Learning Benchmark for Land Use and Land Cover Classification. IEEE J. Sel. Top. Appl. Earth Obs. Remote Sens. 12 (7), 2217–2226.

Hersperger, A.M., Oliveira, E., Pagliarin, S., Palka, G., Verburg, P., Bolliger, J., Grădinaru, S., 2018. Urban Land-Use Change: The Role of Strategic Spatial Planning. Global Environ. Change 51, 32–42.

Hossain, M.F., 2021. Assessment of the Energy Recovery Potential of Waste Photovoltaic (pV) Modules. In: Advanced Technology for the Conversion of Waste into Fuels and Chemicals, pp. 219–238.

Huang, B.o., Zhao, B., Song, Y., 2018a. Urban Land-Use Mapping Using a Deep Convolutional Neural Network with High Spatial Resolution Multispectral Remote Sensing Imagery. Remote Sens. Environ. 214, 73–86.

Huang, R., et al., 2018b. Classification of Settlement Types from Tweets Using LDA and LSTM. In: In *IGARSS 2018–2018 IEEE International Geoscience and Remote Sensing Symposium*, pp. 6408–6411.

Jiang, S., Alves, A., Rodrigues, F., Ferreira, J., Pereira, F.C., 2015. Mining Point-Of-Interest Data from Social Networks for Urban Land Use Classification and Disaggregation. Comput. Environ. Urban Syst. 53, 36–46.

Karim, F., Majumdar, S., Darabi, H., Chen, S., 2018. LSTM Fully Convolutional Networks for Time Series Classification. IEEE Access 6, 1662–1669.

Kussul, N., Lavreniuk, M., Skakun, S., Shelestov, A., 2017. Deep Learning Classification of Land Cover and Crop Types Using Remote Sensing Data. IEEE Geosci. Remote Sens. Lett. 14 (5), 778–782.

Li, L., et al., 2014a. Experiencing and Handling the Diversity in Data Density and Environmental Locality in an Indoor Positioning Service. In: In *Proceedings of the 20th Annual International Conference on Mobile Computing and Networking*, pp. 459–470.
Li, W., Dong, R., Fu, H., Wang, J., Yu, L.e., Gong, P., 2020. Integrating Google Earth Imagery with Landsat Data to Improve 30-M Resolution Land Cover Mapping. Remote Sens. Environ. 237, 111563. https://doi.org/10.1016/j.rse.2019.111563.
Li, X., Myint, S.W., Zhang, Y., Galletti, C., Zhang, X., Turner, B.L., 2014b. Object-Based Land-Cover Classification for Metropolitan Phoenix, Arizona, Using Aerial Photography. Int. J. Appl. Earth Obs. Geoinf. 33, 321–330.
Liu, S., Shi, Q., 2020. Local Climate Zone Mapping as Remote Sensing Scene Classification Using Deep Learning: A Case Study of Metropolitan China. ISPRS J. Photogramm. Remote Sens. 164, 229–242.
Liu, X., He, J., Yao, Y., Zhang, J., Liang, H., Wang, H., Hong, Y.e., 2017. Classifying Urban Land Use by Integrating Remote Sensing and Social Media Data. Int. J. Geogr. Inform. Sci. 31 (8), 1675–1696.
Long, Y., Han, H., Lai, S.-K., Jia, Z., Li, W., Hsu, W., 2020. Evaluation of Urban Planning Implementation from Spatial Dimension: An Analytical Framework for Chinese Cities and Case Study of Beijing. Habitat Int. 101, 102197. https://doi.org/10.1016/j.habitatint.2020.102197.
Marcus, G., 2018. Deep Learning: A Critical Appraisal. *arXiv preprint arXiv:1801.00631*.
Pan, Y., Zeng, W., Guan, Q., Yao, Y., Liang, X., Yue, H., Zhai, Y., Wang, J., 2020. Spatiotemporal Dynamics and the Contributing Factors of Residential Vacancy at a Fine Scale: A Perspective from Municipal Water Consumption. Cities 103, 102745. https://doi.org/10.1016/j.cities.2020.102745.
Queiroz, H., Amaral Lopes, R., Martins, J., 2020. Automated Energy Storage and Curtailment System to Mitigate Distribution Transformer Aging Due to High Renewable Energy Penetration. Electr. Power Syst. Res. 182, 106199. https://doi.org/10.1016/j.epsr.2020.106199.
Rogan, J., Chen, DongMei, 2004. Remote Sensing Technology for Mapping and Monitoring Land-Cover and Land-Use Change. Progr. Plan. 61 (4), 301–325.
Schaetti, N., 2018. Character-Based Convolutional Neural Network and Resnet18 for Twitter Authorprofiling. In: Proceedings of the Ninth International Conference of the CLEF Association (CLEF 2018), Avignon, France, 10–14.
Shen, Y., Karimi, K., 2016. Urban Function Connectivity: Characterisation of Functional Urban Streets with Social Media Check-In Data. Cities 55, 9–21.
Srivastava, S., Vargas Muñoz, J.E., Lobry, S., Tuia, D., 2020. Fine-Grained Landuse Characterization Using Ground-Based Pictures: A Deep Learning Solution Based on Globally Available Data. Int. J. f Geogr. Inform. Sci. 34 (6), 1117–1136.
Srivastava, S., Vargas-Muñoz, J.E., Tuia, D., 2019. Understanding Urban Landuse from the Above and Ground Perspectives: A Deep Learning, Multimodal Solution. Remote Sens. Environ. 228, 129–143.
Su, Y.u., Zhong, Y., Zhu, Q., Zhao, J.i., 2021. Urban Scene Understanding Based on Semantic and Socioeconomic Features: From High-Resolution Remote Sensing Imagery to Multi-Source Geographic Datasets. ISPRS J. Photogramm. Remote Sens. 179, 50–65.
Tasar, O., Tarabalka, Y., Alliez, P., 2019. Incremental Learning for Semantic Segmentation of Large-Scale Remote Sensing Data. IEEE J. Sel. Top. Appl. Earth Obs. Remote Sens. 12 (9), 3524–3537.
Villar-Navascués, R.A., Pérez-Morales, A., 2018. Factors Affecting Domestic Water Consumption On the Spanish Mediterranean Coastline. Prof. Geogr. 70 (3), 513–525.
Wang, J.Q., Du, Y.u., Wang, J., 2020. LSTM Based Long-Term Energy Consumption Prediction with Periodicity. Energy 197, 117197. https://doi.org/10.1016/j.energy.2020.117197.
Wang, Z., Han, Q.i., de Vries, B., 2019. Land Use/Land Cover and Accessibility: Implications of the Correlations for Land Use and Transport Planning. Appl. Spat. Anal. Policy 12 (4), 923–940.
Weng, M., Ding, N., Li, J., Jin, X., Xiao, H.e., He, Z., Su, S., 2019. The 15-Minute Walkable Neighborhoods: Measurement, Social Inequalities and Implications for Building Healthy Communities in Urban China. J. Transp. Health 13, 259–273.
Xia, C., Yeh, A.-O., Zhang, A., 2020. Analyzing Spatial Relationships Between Urban Land Use Intensity and Urban Vitality at Street Block Level: A Case Study of Five Chinese Megacities. Landscape Urban Plann. 193, 103669. https://doi.org/10.1016/j.landurbplan.2019.103669.
Yang, Y., Heppenstall, A., Turner, A., Comber, A., 2019. Who, Where, Why and When? Using Smart Card and Social Media Data to Understand Urban Mobility. ISPRS Int. J. Geo-Inf. 8 (6), 271. https://doi.org/10.3390/ijgi8060271.
Yao, Y., Li, X., Liu, X., Liu, P., Liang, Z., Zhang, J., Mai, K.e., 2017. Sensing Spatial Distribution of Urban Land Use by Integrating Points-of-Interest and Google Word2Vec Model. Int. J. Geogr. Inform. Sci. 31 (4), 825–848.
Yao, Y., Zhang, J., Hong, Y.e., Liang, H., He, J., 2018. Mapping Fine-Scale Urban Housing Prices by Fusing Remotely Sensed Imagery and Social Media Data. Trans. GIS 22 (2), 561–581.
Yao, Y., Zhang, J., Qian, C., Wang, Y.u., Ren, S., Yuan, Z., Guan, Q., 2021. Delineating Urban Job-Housing Patterns at a Parcel Scale with Street View Imagery. Int. J. Geogr. Inform. Sci. 35 (10), 1927–1950.
Ye, C., Zhang, F., Mu, L., Gao, Y., Liu, Y.u., 2021. Urban Function Recognition by Integrating Social Media and Street-Level Imagery. Environ. Plan. B: Urban Anal. City Sci. 48 (6), 1430–1444.
Yin, J., Dong, J., Hamm, N.A.S., Li, Z., Wang, J., Xing, H., Fu, P., 2021. Integrating Remote Sensing and Geospatial Big Data for Urban Land Use Mapping: A Review. Int. J. Appl. Earth Obs. Geoinf. 103, 102514. https://doi.org/10.1016/j.jag.2021.102514.
Yuan, Q., Shen, H., Li, T., Li, Z., Li, S., Jiang, Y., Xu, H., Tan, W., Yang, Q., Wang, J., Gao, J., Zhang, L., 2020. Deep Learning in Environmental Remote Sensing: Achievements and Challenges. Remote Sens. Environ. 241, 111716. https://doi.org/10.1016/j.rse.2020.111716.
Zhan, X., Ukkusuri, S.V., Zhu, F., 2014. Inferring Urban Land Use Using Large-Scale Social Media Check-In Data. Netw. Spat. Econ. 14 (3-4), 647–667.
Zhang, J., Li, X., Yao, Y., Hong, Y.e., He, J., Jiang, Z., Sun, J., 2021. The Traj2Vec Model to Quantify Residents' Spatial Trajectories and Estimate the Proportions of Urban Land-Use Types. Int. J. Geogr. Inform. Sci. 35 (1), 193–211.
Zhang, X., Du, S., Wang, Q., 2017. Hierarchical Semantic Cognition for Urban Functional Zones with VHR Satellite Images and POI Data. ISPRS J. Photogramm. Remote Sens. 132, 170–184.
Zhang, Y., Li, Q., Tu, W., Mai, K.e., Yao, Y., Chen, Y., 2019. Functional Urban Land Use Recognition Integrating Multi-Source Geospatial Data and Cross-Correlations. Comput. Environ. Urban Syst. 78, 101374. https://doi.org/10.1016/j.compenvurbsys.2019.101374.
Zhang, Z., Wang, X., Zhao, X., Liu, B., Yi, L., Zuo, L., Wen, Q., Liu, F., Xu, J., Hu, S., 2014. A 2010 Update of National Land Use/Cover Database of China at 1: 100000 Scale Using Medium Spatial Resolution Satellite Images. Remote Sens. Environ. 149, 142–154.